Session 2A3
New Applications of Radar for Non-destructive Testing

Detection of Groundwater by Ground Penetrating Radar

S. I. Elkhetali
Academy of Graduate Studies, Libya

Abstract—The application of ground probing radar (GPR) to detection of groundwater from relatively deep aquifers in a desert environment is addressed and processing techniques to improve the detectability of a weak signal in noise and interference are reported. The study is based on simulated images from structures that have the potential of storing groundwater one of which is the buried valley structure.

To increase the signal to noise ratio to achieve a reasonable probability of detection and false alarm, various processing schemes are possible, typically employing analogue, binary (double threshold) and digital processing. Different system architectures are compared to improve detectability. Automatic detection and classification by artificial neural networks is tried to classify geologic subterranean features for aiding and speeding the process and to overcome lack of experts on the field.

1. Introduction

Figure 1 shows how losses increase with depth. Losses include attenuation, spreading losses and loss due reflection coefficient from the buried interface. The bottom layer is considered to be saturated soil giving a reflection coefficient of 0.25. Losses that depend on external influences and not on system parameters are lumped together and called external losses, they are expressed as follows.

$$Loss = \frac{\lambda^2 \sigma |\rho|^2 e^{-4\alpha R}}{(4\pi)^3 R^4} \tag{1}$$

where λ is the wavelength, σ is the scattering cross section, ρ is the reflection coefficient and R is the interface depth. For a planar interface the scattering cross section is given as $\sigma = \frac{\pi \lambda R}{4}$, which is the first Fresnel zone [1].

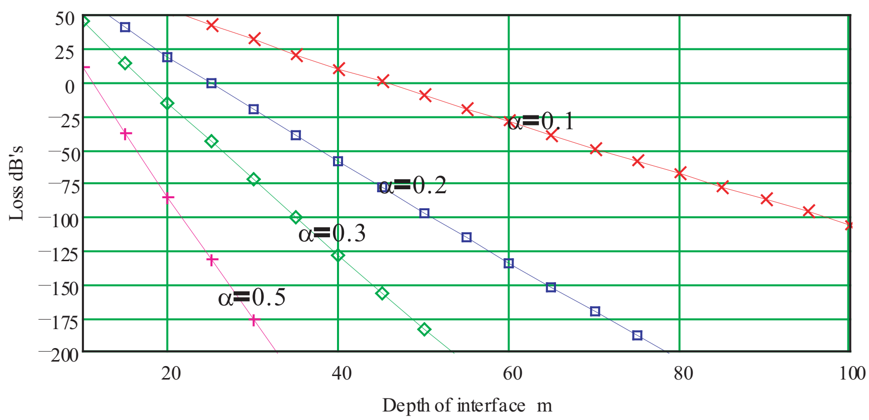

Figure 1: A monogram showing how losses increase as functions of depth and attenuation.

2. System comparison

Different detection techniques are compared. The processors that are compared are digital, binary and step frequency.

2.1. Digital Pulsed System

This is a pulsed radar having a digital processor assuming the use of swept gain amplifier which compensates for attenuation due to the range of each scatterer.

The system gain before digitisation is chosen so that interference and noise would not exceed the input range of the ADC full scale ratio (FSR) for an acceptable time duration (implying a large probability that the interference is within the FSR). Assuming that the input to the ADC is Rayleigh distributed. If the FSR to be equal to 10 σ implies saturation for only 1% of the time. The amplification factor satisfying the 1% saturation criterion is 48 dB (for a FSR=10 V) and 23 dB (for a FSR of 0.54 V).

The noise level without amplification is -64 dBm and the interference power is -34 dBm and if the bandwidth is increased to 20 MHz (a pulse duration of 0.05 μs) the noise will be -61 dBm and interference will be -31 dBm. It is seen that interference is the dominant factor and therefore the time required to increase the output signal to noise ratio for the digital processing would be equivalent to that of an analogue system. Therefore, an 8 bit ADC would probably be adequate.

Table 1: Quantisation noise and amplified input noise and interference.

FSR, V	Quantisation noise for an ADC with the number of bits in dBm			applied gain dB	amplified noise dBm	amplified interference dBm
	8 bits	10 bits	12 bits			
10	-9	-21	-33	48	-16	13.2
0.54	-34.3	-46	-58	23	-41	-12.3

2.2. Pulsed Radar System with Binary Integration

The binary integrator has a threshold device that generates 1's or 0's depending on whether the input to the device has exceeded a certain threshold voltage or not. After detection noise alone has a Rayleigh probability density function and the sum of the signal and noise has a Rician probability density function.

The next summing device taking the input from the threshold device will count the number of 1's obtained from a collecting a set of pulses. If the total exceeds a certain number (k out of m) which is a type of (digital) threshold, a target is declared. The input to the threshold device has a signal to noise ratio defined as the ratio of signal voltage to standard deviation of the noise and is given the symbol a, [1].

The signal to noise ratio of the quantised video is defined as $\rho = \frac{p_s - p_n}{\sqrt{p_n(1-p_n)}}$, where p_n is the probability of obtaining a quantised pulse (binary 1) due to noise alone and p_s is the probability of obtaining a quantised pulse when the signal is present. The signal to noise ratio of integrated video is $SNR_{out} = \sqrt{m}\,\rho$ where m is the number of integrated pulses. For an input signal to noise ratio of - 37 dB (his is when assuming the radar has a transmitted power of 10 w and a pulse duration of 0.05 μs) $\rho = 8{\times}10^{-5}$ for input $SNR = -37$ dB, $m = \left(\frac{SNR_0}{\rho}\right)^2$, making the number of pulses that are needed for integration to be about $4{\times}10^9$. The output SNR being 7 dB. The time to collect data is about 22 hours for a prf of 50 kHz.

The choice of the second threshold k out of m is

$$k = SNR_{out}\sqrt{m}p_n(1-p_n) + mp_n + \frac{1}{2} \tag{2}$$

Therefore, k is 8×10^8 and so if the number of 1's exceeds 8×10^8 then a target is declared.

2.3. A Step Frequency Processor.

The radar system transmits a sinusoid and measures the magnitude and the phase angle of the received signal. It does this for a group of sinusoids forming the spectral components of the time domain signal that we want to synthesise and then an IDFT is performed to obtain the reflected signal in the time domain. This must be the point of comparing data obtained by the step frequency and the pulsed radar systems. At the input to the display device the value of signal to noise ratio must 7 dB to have the same probabilities of detection and false alarm as that of the pulsed system. The step frequency (SF) radar can be operated with an instantaneous narrow bandwidth making the input noise and interference to remain low and therefore quantisation noise may become dominant.

2.3.1. A radio Frequency Digitising System

Figure 4 presents a step frequency system digitising the signal at radio frequency.

A step frequency radar system with a system noise factor of 10 is considered, a transmitted power of 1 W, a bandwidth of the preselector filter of 1 kHz, a pulse duration of 1 ms and a burst repetition frequency of 1 kHz. The number of frequency spectral samples is 40 (20 MHz effective bandwidth with a frequency step of 0.5 MHz). The signal to noise ratio at point A is the thermal noise is $kTFB = -134$ dBm and the atmospheric noise (being 30 dB above thermal) is -104 dBm. Interference power is -75 dB (not allowing for low interference bands) and if low interference bands are utilised, it would be about -115 dBm (the power spectral density of interference in these bands is about -145 dBm/Hz).

The number of bursts that has to be collected and integrated is determined by the need to bring the signal to noise ratio at point C to that is required at point D. Considering an ADC having 8 bits and an FSR of 10 V, the signal to noise ratio at point C would be -71 dB. The number of bursts that are needed for integration is about 6.4×10^6. The integration is coherent and so it is assumed to have an improvement that is $\propto N$. If the FSR is made 0.54 V with an 8 bit ADC and no gain is applied, the number of bursts that are needed for integration are 2×10^4 and the total time to collect all the data is about 13 minutes.

The signal to noise, interference and quantisation ratio at point B is $\mathrm{SNIQR} = \frac{\mathrm{Pr} \cdot \mathrm{G}}{(\mathrm{Na+I}) \cdot \mathrm{G} + \mathrm{Nq}}$.
where Na is atmospheric noise power, I is interference power, Nq is quantisation noise power and G is gain.

For $FSR = 10$ V, the gain that may be applied before clutter saturates the ADC is about 7 dB. The signal to total noise ratio (total including noise interference and quantisation noise) is -63 dB, the number of pulses to be integrated is about 9×10^5. If the ADC has 10 bits, the time would be about 40 minutes and for a 12 bit ADC the time would be about 3 minutes. It seems that quantisation noise is higher than input noise and interference in the case of a SF radar.

2.3.2. A Proposed System

The radar system presented in Figure 4 digitises at the radio frequency which is possible at HF but if the radar operates at higher frequencies it may be difficult. There are many designs to make the ADC's work at lower frequencies by implementing a mixer to down convert the frequency either to DC or to other IF's higher than zero, all of which suffer from the inherent drawbacks of the analog components. A proposed system avoiding these problems and does not require the ADC's to work at excessively high frequencies is given in Figure 5. The system is composed of four ADC's working in an interleaved manner. The timing of sampling between the samplers is T/4, T is the period of the received signal.

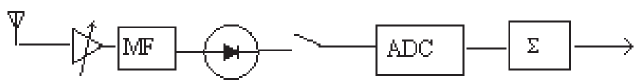

Figure 2: A pulsed digital processor.

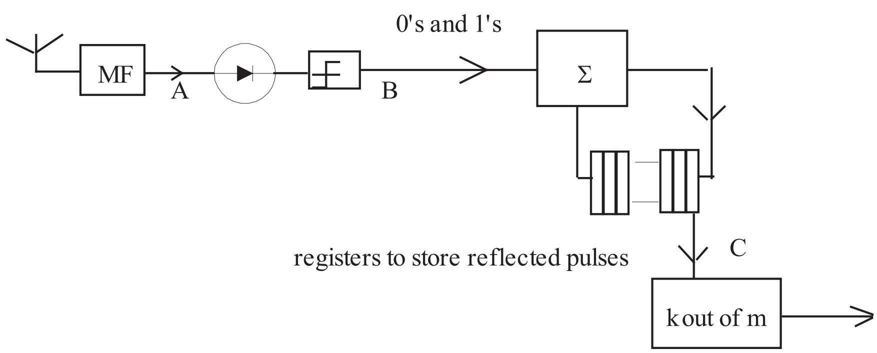

Figure 3: A pulsed system with a binary integrator.

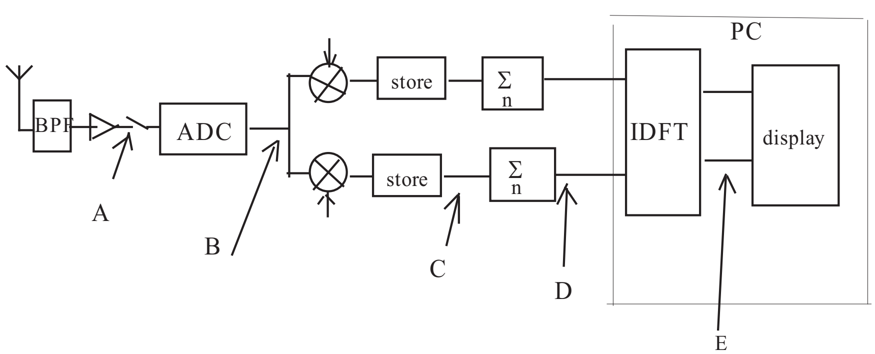

Figure 4: A step frequency processor with RF digitisation.

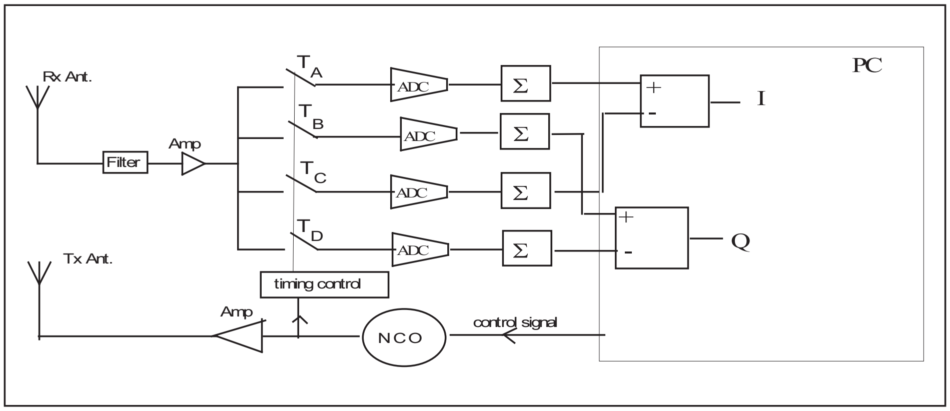

Figure 5: Schematic diagram of the proposed radar system.

2.3.3. Measurement of Amplitude and Phase Angle of a Sinusoid

The magnitude and phase of the received signal is gives by the following equations.

$$\text{Magnitude} = \frac{\sqrt{I^2 + Q^2}}{2} \quad \text{and the} \quad \text{Angle} = \tan^{-1}\left(\frac{-Q}{I}\right) \tag{3}$$

Figure 6 show a simulated traces and an image as obtained by the radar.

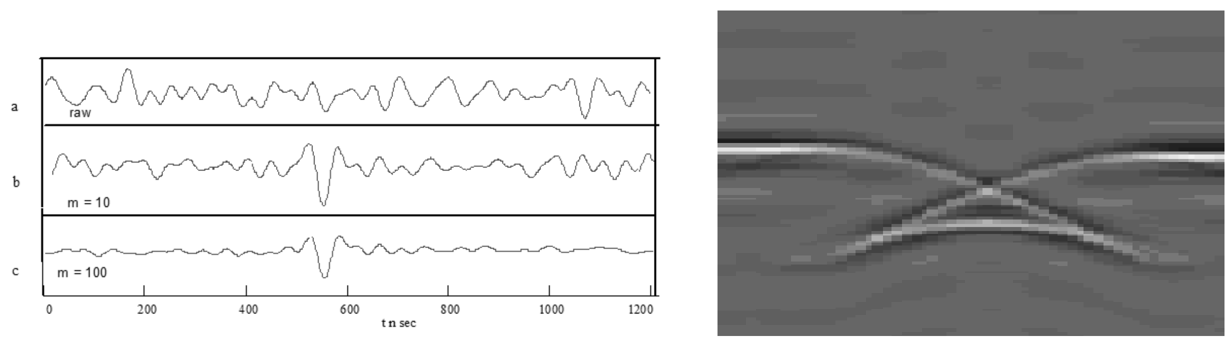

(a) (b)

Figure 6: a) Signals after averaging repeated samples. (m is the number of averaged samples) and b) The radar image of a buried channel.

3. Artificial Neural Networks

Samples of the simulated images that were fed to the ANN's for classification are shown in Figure 7. The size of the images is 80 by 50 pixels. The structures are those of, mostly, a buried valley having different cross section shapes one of which is having a saturated zone. Another image is of a buried dome structure.

A backpropagation artificial network is used fro image classification. Results provided are for the conditions of number of neurons in the middle layer being 10, sum square error is 0.1 and the SNR is 10 dB. It is found that the ANN classifier gives very high success rate.

4. Summary and Discussion

It is seen that binary integration takes longer time than analogue but it has a small word length making it simpler to implement and being low cost. Because of its simplicity, it may be possible to operate the binary integration scheme at higher prf's, allowing the time of data collection to be reduced. The Step frequency radar may operate with powers that are lower than those needed for a pulsed radar and takes shorter time to acquire the data. For SF radar, the averaging of many samples of the signal increases the SNR coherently. ANN's are useful in classifying the subterranean images.

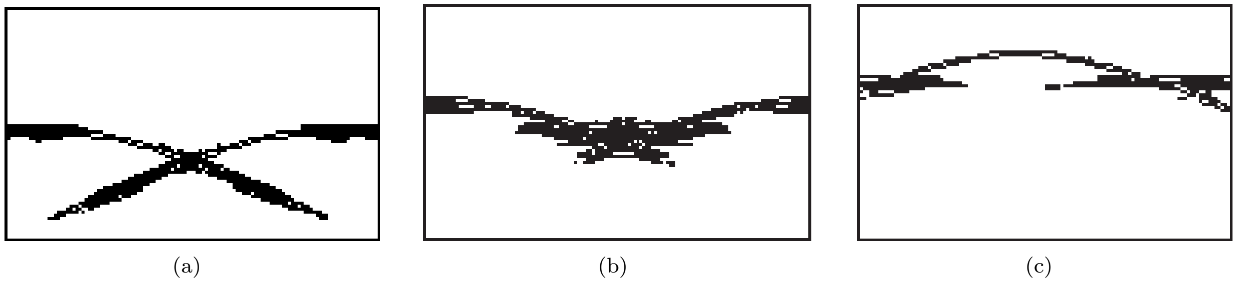

Figure 7: Samples of some images of the geological features that are used for the ANN's.

REFERENCES

1. Elkhetali, S. I., "Application of ground probing radar for detection of groundwater in arid regions," PhD Thesis, School of Electronic and Electrical Engineering, University of Birmingham, UK, 1998.
2. Goodman, D., "Ground penetrating radar simulation in engineering and archaeology," *Geophysics*, Vol. 59, No. 2, 224, 1994.
3. Jol, H. M., "A comparison of the 25, 50, 100, and 200 MHz with 400 and 1000 v transmitters : a ground penetrating radar field study," *54th Meeting of the E. A. E. G. and Technical Exhibition*, Paris, 1–5 June, 1992.
4. Ulaby, F. T., R. K. Moore, and A. K. Fung, *Microwave Remote Sensing; Active and Passive*, Addison-Wesley, Reading Mass. USA, 1981.
5. Yilmaz, O., *Seismic Data Processing, Society for Exploration Geophysicists*, Tulsa, Ok., 1987.

Detection of Buried Objects in Periodic Structures with Ground Penetrating Radar Mounted on Moving Vehicles

P. Falorni, L. Capineri, and L. Masotti
University of Florence, Italy

C. G. Windsor
116, New Road, East Hagbourne, OX11 9LD, UK

The aim of this paper is the analysis and the development of algorithms capable to detect anomalies in periodic structures by using an ultra-wide-band (UWB) Ground Penetrating Radar. These inspection methods based on GPR are commonly used for surveys of civil structures like rebar underneath a road or a bridge or more recently for landmines detection along railway tracks. In these cases a radar with an array of antennae is generally mounted on a moving vehicle which allows the acquisition of radar signals at a certain velocity. In order to detect variations of the inspected area in real time it is necessary to develop quick signal processing methods also capable to account for the unavoidable variation of the background measurable with radar (e.g., period of the bars distance in the railway or the thickness of a layer in a road).

Among several possible methods available in the literature (physical model based or image processing based) we decide for the homomorphic deconvolution of radar signal based on the Cepstrum [ref 1]. This technique has been chosen according to the assumption that the received radar signal is generated by the convolution of the transmitted signal and the characteristic function of the object. To prove this assumption we synthesized signals of some buried landmines with the convolution model and we compared with the experimental one. In the case of the rebar or pipes buried in concrete layers, this assumption is still valid considering that the radar central wavelength is much comparable to the object size and the characteristic object function becomes simpler. This trial on simple objects was needed to set the algorithm parameters. Then we have simulated several cases of interest for GPR surveys like variation of object dimensions, variation of the periodic pattern, variation of the periodic buried objects lateral distance and different values of signal to noise ratio. The method included a moving window approach to calculate variations in the acquired signals and requires an initialization step (initial pattern estimation). Other methods based on Fourier Transform have also been investigated.

Finally the algorithm was applied to an experimental dataset of rebar buried in a 4 cm thick concrete layer separated by 12 cm. The signals are acquired in a bridge with a 1.5 GHz central frequency UWB radar along a distance of 7 m. The results are an average distance of rebar 15.5 cm with standard deviation 2.3 cm. A processing time of 0.5 s with acquisitions at pulse repetition frequency of 32 kHz was found to be compatible with a vehicles velocity of about 6 km/h.

REFERENCES

1. Oppenheim, A. V. and R. W. Shafer, *Digital signal processing*, Prentice Hall, London, 1975.

Development of High Speed GPR for Railtrack Assessment

S. Bandyopadhyay[1], **J. Gascoyne**[2], and **W. Al-Nuaimy**[1]
[1]University of Liverpool, UK
[2]Zetica, UK

Rapid and non-destructive evaluation of the quality of the railway infrastructure, specifically the under-track ballast, is a growing concern worldwide, and GPR has demonstrated its ability to provide such an evaluation, within the constraints of the available technology. This paper presents the results of ongoing research into the development of a high-speed train-mounted multiple-antenna GPR system for non-destructive assessment of the railway trackbed. By travelling on trains in service and at line speeds, such an inspection system can significantly improve the efficiency and cost-effectiveness of maintaining and renewing railway under-track ballast. The paper addresses the issues of antenna shielding against electromagnetic interference, electromagnetic compatibility tests, antenna choice, configurations and positioning, as well as optimal methods for triggering, registration, and post-processing.

Methods for triggering an array of GPR antennas and transferring control between multiple systems are investigated and detailed, as are techniques for coordinating different data sets, namely, multi-frequency GPR arrays, multiple video sequences, GPS positioning data, GIS location data and other track data, in order to fuse the data layers both before and after interpretation within the existing rail model. The paper further details the design and implementation of the control units, the GPR event marker system and data fusion layers prior to processing and interpretation. Results are resented from the UKs first high-speed (60 mph) train-mounted GPR trials.

Automatic Processing of Train-mounted GPR Data for Ballast Inspection

A. Doshi and W. Al-Nuaimy
University of Liverpool, UK

Until very recently, inspection of railtrack using high-speed GPR was not possible due to hardware technology limitations. With the development of newer and faster GPR systems, the prospect of high-speed GPR inspection of rail ballast has become very real, and there is increased interest in developing interpretation algorithms capable of dealing with the large volumes (typically gigabytes) of GPR data that result from such surveys. Such computational tools are required to process and interpret the multi-channel GPR data in a robust, consistent and reliable manner, and present the results in a manner consistent with industry expectations and regulations.

This paper presents recent developments towards new GPR data interpretation software enabling fast, reliable and automated processing of multiple data sets of unlimited size. Specifically, algorithms have been designed for processing the GPR data to reduce the effect of background and clutter using novel signal and image processing techniques. Techniques have been formulated for minimising/ eliminating the effect of sleepers (steel and concrete) on high speed rail GPR data. Interactive semi-automated layer picking routines have been designed for pinpointing the ballast-subgrade interface, and for identifying surface anomalies such as AWS magnets and footbridges. Automated and semi-automated methods are presented for ballast dielectric modelling based on the data interpretation and any available corroborative information such as core samples. This allows automatic depth calibration and profiling. Finally, pattern recognition techniques have been been developed to characterise spent or fouled ballast from clean ballast, and have been employed in conjunction with neural networks to automatically characterise the quality of the ballast sub-track by determining the level and nature of degradation in ballast. Results are presented from a number of high-speed trials in the UK.

Frequency and Time Domain Error in Buried Target Radar Signature Extraction

I. van den Bosch[1], P. Druyts[1], M. Acheroy[1], and I. Huynen[2]

[1]Royal Military Academy, Belgium
[2]Microwaves and Communications laboratory, Belgium

The ground-penetrating radar (GPR) model developed by van den Bosch et al., [1] allows for the extraction of the target radar signature, in theory free from the antenna signal artifacts (internal re ections, emission and reception equivalent currents amplitudes and the multiple re ections) and from the soil response. For this, the radar system has to be characterized for determining the antenna operational parameters H_i (antenna internal re ections), H_t^2 (antenna transmission and reception) and H_f (antenna scattering), and a measurement above the soil without the target has to be performed in order to extract its radar signature R_S. With this in hand, one is able to recover the target signature R_T by using the method developed in [1], where comparisons between extracted and computed target signatures have been made, and excellent agreement has been found.

However, real world conditions are far from the laboratory settings in which the experiments were performed. The operational parameters of the antenna can be wrongly estimated. In our experience, these parameters are strongly dependent upon the strength with which the waveguide is attached to the VNA. On another hand, the soil EM parameters, namely the dielectric permittivity and magnetic permeability, can—and do—vary greatly from point to point, therefore an estimation of those parameters or of R_S may not correspond to the reality of the ground surrounding the buried target.

In this work, the relative error on the target signature is decomposed into a weighted sum of the relative errors on the terms that participate to the total radar signal. It is shown how the frequency domain magnitudes of these weights are inversely proportional to the magnitude of the target signature. Special attention is devoted to the error due to wrong soil radar response estimation. Its consequences are thoroughly examined in the time domain, which allows for an intuitive yet rigorous interpretation of the resulting degradation of target discrimination against the background.

REFERENCES

1. Van den Bosch, I., P. Druyts, S. Lambot, I. Huynen, and M. Acheroy, "Accurate and efficient modeling of monostatic GPR signal of dielectric targets embedded in stratified media," *Proceedings of the Progress in Electromagnetics Research Symposium (PIERS)*, 251–255, Hangzhou, Zhejiang, China, August 2005.

GPR Ground Bounce Removal Methods Based on Blind Source Separation

J.-X. Liu, **B. Zhang**, **and R.-B. Wu**
Civil Aviation University of China, China

Abstract—In this paper, the ground bounce (GB) removal methods based on Blind Source Separation (BSS) for land mine detection using ground penetrating radar (GPR) are investigated. These methods include an Independent Component Analysis (ICA) based method and Blind Instantaneous Signal Separation (BISS) based method. First, a modified ICA based method is presented. In this method, a fully automatic eigenimage based Independent Components (ICs) selection strategy combined with a non-homogeneous detector (NHD) is introduced. A BISS based method is also proposed for the GB removal. This method can be applied in various environments as ICA, but it has much fewer number of extracted components than ICA's, but has much fewer number of components to extract, therefore less computation load is required. Experimental results show that the proposed methods exhibit good performance.

1. Introduction

Downward looking GPR has been considered a viable technology for land mine detection [1]. For GPR with the antenna positioned very close to the ground surface, the reflections from the ground surface, i. e., the GB, are very strong and can much dominate the weak returns from shallowly buried plastic mines. Hence, one of the key challenges of using GPRs for landmine detection is to remove the GB as completely as possible without altering the landmine return.

The literature suggests a number of clutter (whose dominant contributor is GB) reduction methods, such as parametric system identification [2, 3], wavelet packet decomposition [4], subspace techniques [5, 6], and simple mean subtraction [7]. However, many of these fail to detect shallowly buried landmines, mostly because of the statistical nature of the clutter, e.g., the ground surface is not perfectly flat nor even relatively smooth. The other problem is that many of the methods use reference signals to estimate the signature of a landmine. These reference signals are used to remove signals based on how they relate to the reference. This will lead to improper target signal cancellation when the reference signals are selected inadequately. For subspace techniques, the GPR signals are decomposed into clutter and landmine signals by selecting principal components (PCs) and independent components (ICs) reasonably. These methods can be more robust and lead to the best results for GB removal. But automatic selection strategy for PCs and ICs is the key problem, and reduction for computational load is an attractive work.

In this paper, we present an NHD-based modified ICA algorithm with automatic selection strategy for PCs and ICs. To reduce the computational load, we also apply NHD to BISS to determine the number of components to be extracted.

2. Data Description

Consider a stepped frequency GPR system moving in the along-track direction. Let $x_p(\omega_n)$ denote the data collected at the pth scan for the nth stepped frequency, $b_p(\omega_n)$ denote ground bounce in $x_p(\omega_n)$, where $\mathbf{x}_p = [x_p(\omega_1)x_p(\omega_2)\cdots x_p(\omega_N)]^T$ is called A-scan data vector (for impulse GPR radar, this is the data vector expressed in the frequency domain), $\mathbf{b}_p = [b_p(\omega_1)b_p(\omega_2)\cdots b_p(\omega_N)]^T$ represents the ground bounce vector, and $\mathbf{X} = [x_1x_2\cdots x_p]$ represents the B-scan data matrix. As the mutual coupling of antennas can be removed by prior measurement or estimation, the received data vector at the pth scan can be simplified as

$$\mathbf{x}_p = \mathbf{r}_p + \mathbf{b}_p + \mathbf{e}_p \tag{1}$$

where $\mathbf{r}_p$ denotes reflected signal form target, and $\mathbf{e}_p$ denotes un-modeled noise. We also set up a sliding window for modified GLR-based HND [8], which is composed of a guard area of length N_1 and local area of length N_2 in the along-track direction[8, 9].

3. Modified ICA Based Method

3.1. Temporal ICA

The temporal ICA is one of the subspace techniques to remove GPR GB. The received signal is considered as the linear mixture of the independent components (ICs) [5, 6], and the GB is removed by reconstructing received signal with ICs corresponding to landmine target and target-like objects. ICA algorithm is processed in two steps. The first step is the pre-processing, which includes data centralization ($\mathbf{x}_{m,j} = \mathbf{x}_j - (1/P)\sum_{i=1}^{P}\mathbf{x}_i, j = 1 \sim P$) and whitening. The whitening is realized by PCA ($\mathbf{X}_m = [\mathbf{x}_{m,1}\cdots\mathbf{x}_{m,P}]$, $\mathbf{X}_1 = \mathbf{X}_m^T$, $\mathbf{Y} = \tilde{\mathbf{U}}^T\mathbf{X}_1$), where $\mathbf{y} = [y_1 y_2 \cdots y_{L_1}]^T$ is constructed by L_1 selected PCs, and $\mathbf{U}$ is the projection matrix for $\mathbf{X}_1$ projected in a subspace spanned by eigenvectors of L_1 selected PCs. Then, we consider $\mathbf{Y}$ as the input of ICA defined as

$$\mathbf{Y} = \mathbf{AS} = [\mathbf{a}_1\mathbf{a}_2\cdots\mathbf{a}_{L_1}][s_1 s_2\cdots s_{L_1}]^T = \sum_{i=1}^{L_1} a_i s_j^T \tag{2}$$

$$\mathbf{X}_1 = \tilde{\mathbf{U}}\mathbf{Y} = \tilde{\mathbf{U}}\mathbf{AS} = \mathbf{WS} = [\mathbf{w}_1\mathbf{w}_2\cdots\mathbf{w}_L]\mathbf{S} = \sum_{i=1}^{L_1}\mathbf{s}_i\mathbf{w}_i^T \tag{3}$$

where $\mathbf{W}$ is called matrix of eigenimages, and $\mathbf{S}$ is the ICs. After selecting K target and target-like ICs $s_{o,i} = s_j(i = 1 \sim K,\ j = 1 \sim L_1)$ and correspondent eigenimages $\mathbf{w}_{o,i} = \mathbf{w}_j(i = 1 \sim K)$, the GB removal output is $\hat{\mathbf{X}}_I = \sum_{i=1}^{K}\mathbf{s}_{o,i}\mathbf{w}_{o,i}^T$. The key problem for ICA is how to select PCs for PCA and ICs for signal reconstruction.

3.2. PCs and ICs Selection Strategy

The PCs and ICs reflect the time-domain information and the eigenimages can be considered as the spatial steering vectors correspondent to them. The result of the NHD describes the buried position of the targets and target-like objects. So we can select PCs and ICs automatically according to the consistency between the eigenimage and the output of the modified GLR-based HND [8].

4. BISS Based Method

4.1. BISS

The ICA will be very computational demanding if the number of source signals is large [10–12]. After PCA, $L_1 \ll P$, but $L_1 \gg M$ (the number of targets and target-like objects). Obviously, ICA extracts much more signal the sources than that need by signal reconstructing. Fortunately, BISS overcomes somewhat this difficulty. The spirit of the BISS is to recover only a small subset of sources from a large number of sensor signals. For GB removal, if the number of targets and target-like objects is prior known, source signals not more than M are needed to be extracted.

Like the ICA, the first step of BISS is pre-processing. Then, the small subset of targets signals $\mathbf{S}_t$ is extracted from $\mathbf{Y}$ as

$$\mathbf{S}_t = \mathbf{HY} \tag{4}$$

where $\mathbf{H}$ is the separating matrix, and the GB removal output is

$$\hat{\mathbf{X}}_{\mathbf{BISS}} = \mathbf{W_t S_t} = \tilde{\mathbf{U}}\mathbf{H^T S_t} \tag{5}$$

The presented BISS algorithm is gradient-based algorithm that optimizes three different criteria: Maximum Likelihood (ML), Minimum Entropy (ME) and Cumulants based index. The algorithm based ML can be explicitly computed only when the sources densities are known. It needs to approximate the activation function for ME, although it is not necessary to know the source densities. The most robust approach is the cumulant-based algorithm, since it can be realized without approximations and not dependent on the density of sources [11].

4.2. Determination of M and Cumulant Order

There are two important parameters to be conformed for cumulant-based algorithm [13]: the number of extracted signals M and the order of the cumulant. Since the location of target, target-like object, and the homogeneity of GB can be detected by modified GLR based NHD, the value of M can be prior determined, and the order of cumulant should be chosen according to the statistical nature of GPR data.

5. Experiment Result

The GPR data is obtaied from Vrije Universiteit Brussel (VUB) [14]. The experiment was performed in wet clay mixed with small rocks. An area of $x = 50$ cm by $y = 196$ cm was scanned with a scanning step of 1 cm in each direction. There were irregularities with a maximum of 10 cm between the highest and the lowest point. The antenna head was placed at 5 cm above the highest point, and the scan was done horizontally. In

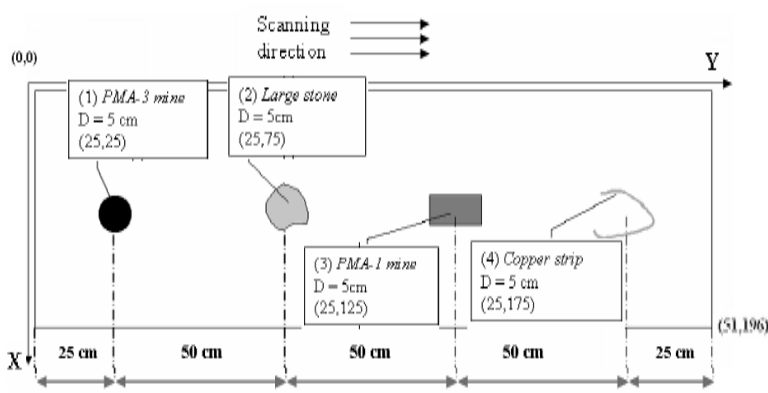

Figure 1: Distribution of buried objects.

the following examples, the target is a plastic anti-personal mine (PMA-1·PMA-3), big stone and curving U shape copper strip, the distribution of buried object is shown in Figure 1.

Figure 2 shows the output of the modified GLR base NHD. Using this result, the number and position of the targets (and target-like objects) can be determined.

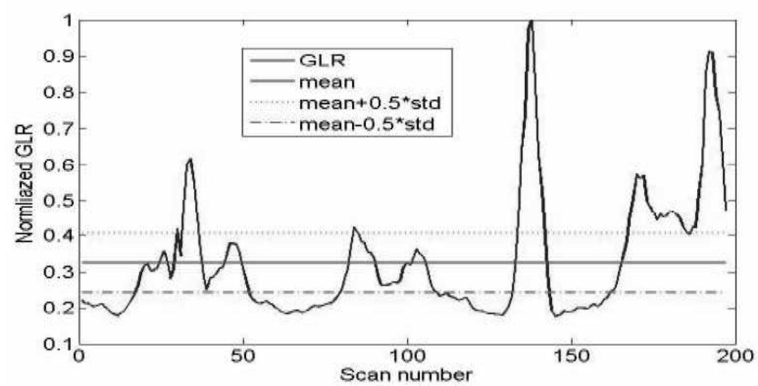

Figure 2: Output of normalized GLR.

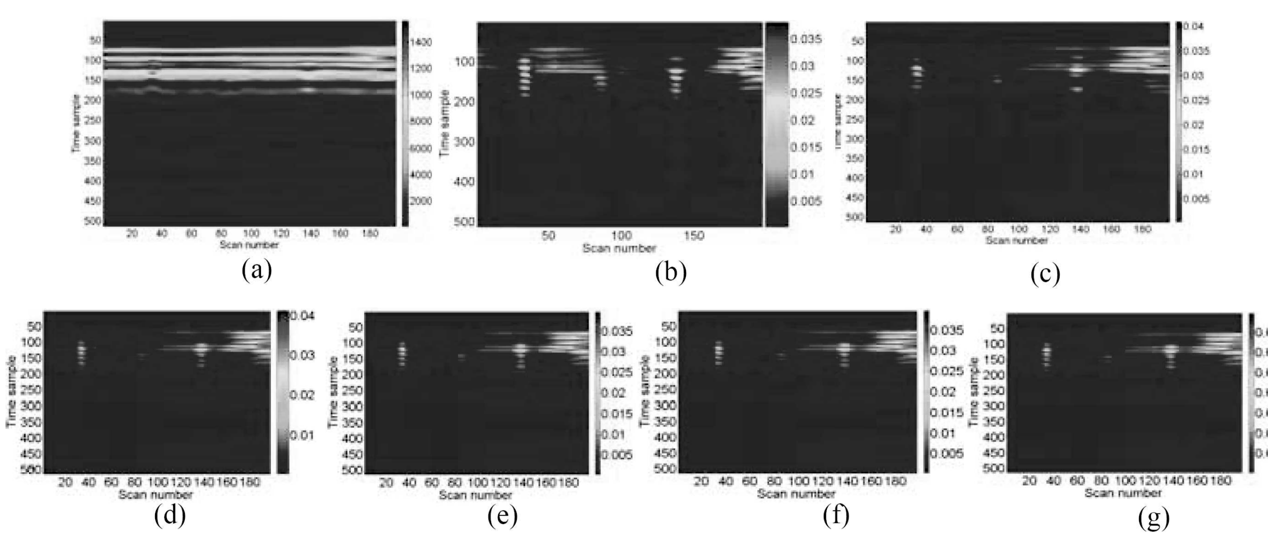

Figure 3: Comparison of ground bounce removal performances. (a) raw data, (b) ICA, (c) NHD based ICA, (d)BISS based 3rd order cumluant, (e) BISS based 4th order cumluant, (f) BISS based 3rd and 4th order cumluant, (g) BISS based 3rd, 4th, 5th, and 6th order cumluant.

The performance of the improved ICA and BISS based method are showed in the Figure 3. Figure 3(a) is the original received data of the GPR. It can be seen that the targets are obscured by the ground bounce. Figure 3(b) and Figure 3(c) show the results of ICA and NHD based ICA, respectively. Figure 3(d)∼(g) shows the results of BISS based cumluants with different orders. It can be seen that there are almost no difference among these four results, so the third order cumluant is enough.

5. Conclusion

In this paper, we present NHD-based ICs selection method. ICA can be realized automatically with this selection strategy. We also apply the BISS in the GB removal combined with NHD to determine the number of extracted signal sources. The experimental results show that these two methods have excellent performance in GB removal, and the BISS based method reduces the computational load greatly.

Acknowledgements

This work was supported by the National Natural Science Foundation of China under grant 60272049 and 60325102, and by the Natural Science Foundation of Tianjin under grant 023601511.

REFERENCES

1. Witten, T. R, "Present state-of-art in ground penetrating radars for mine detection," *Proc. SPIE*, Vol. 3392, 576–586, 1998.
2. Der Merwe, A. V. and I. J. Gupta, "A novel signal processing technique for clutter reduction in GPR measurements of small, shallow land mines," *IEEE Trans. Geosci. Remote Sensing*, Vol. 38, 2627–2637, November 2000.
3. Brooks, J., L. van Kempen, and H. Sahli, "A primary study in sdaptive teduction and buried minelike target enhancement from GPR data," *Proc. SPIE, Detection and Remediation Technologies for Mines and Minelike Targets*, Vol. 4038, Orlando, Florida USA, 1183–1192, August 2000.
4. Carevic, D., "Clutter reduction and target detection in ground penetrating radar data using wavelet packet transform," *Proc. Of IEEE Int. Ant. and Propaga. Soc. Symp.*, Vol. 3, 1780–1783, 1999.
5. Karlsen, B., J. Larsen, K. Jakobsen, and S. Abrahamson, "Antenna characteristics and air-ground interface deembedding methods for stepped-frequency ground penetrating radar measurements," *Proc.of SPIE, AeroSense 2000*, Vol. 4038, April 2000.
6. Karlsen, B., H. B. D. Søensen, J. Lanrsen, and K. B. Jakobsen, "Independent component analysis for clutter reduction in ground penetrating radar data," *SPIE*, Vol. 4742.
7. Brunzell, H., "Detection of shallowly buried objects using impulse radar," *IEEE Transactions on Geoscience and Remote sensing*, Vol. 37, 875–886, March 1999.
8. Liu, J.-X., R.-B. Wu, T. Li, H.-Y. Li, B. Zhang, and J.-X. Huang, "Reference data selection for ground bounce removal with ground penetrating radar," *Proc.of IRS 2005*, Berlin Germany, 783–787, 6–8 September 2005.
9. Wu, R., A. Clement, J. Li, E. G. Larsson, M. Bradley, J. Habersat, and G. Maksymonko, "Adaptive ground bounce removal," *ELECTRONICS LETTERS*, Vol. 37, No. 20, 1250–1252, September 27, 2001.
10. Alvarez, S. A. C., A. Cichocki, and S.-I. Amari, "From blind signal extraction to blind instantaneous signal separation: criteria, algorithms, and stablility," *IEEE transactions on neural network*, Vol. 15, No. 4, July 2004.
11. Alvarez, S. A. C., A. Cichocki, and S.-I. Amari, "On a new blind signal extraction algorithm: different criteria and stability analysis," *IEEE signal processing letters*, Vol. 9, No. 8, August 2002.
12. Cruees, S., A. Cichocki, and S.-I. Amari, "Criteria for the simulateous blind extraction of arbitrary groups of sources," *The 3rd International Conference on Independent Component Analysis and Blind Signal Separation. SanDiego*, Callifornia, USA, 2001.
13. Amari, A. C. S., K. Siek, et al., ICALAB Toolboxed. [Online] URL: http://www.bs.branin.riken.go.jp-/ICALAB, 2003.
14. Vrije Universiteit Brussel(VUB) http://www.minedet.etro.vub.ac.be.

Detection and Characterization of Targets Buried Below a Rough Surface

K. Belkebir, **O. Cmielewski**, **A. Litman**, **M. Saillard**, **and H. Tortel**
CNRS, France

The problem of detection and characterization of an object buried at very low depth beneath a rough surface is addressed. At least two approaches have been proposed to solve such an inverse problem. One of them consists in reconstructing simultaneously both the scatterer and the surface profile. One can also proceed in two steps: first, the surface profile is reconstructed from the early-time response to ultra-wide band signals, and the corresponding Green's function is built numerically. The second step deals with the reconstruction of a scatterer embedded in a (rough) stratified medium. However, both methods assume that the buried object has been previously detected and localized, since only a small area around the scatterer is considered. Here, the whole signal processing scheme is described, from detection to inversion, assuming that a multi-static and multi-frequency data set is available, from measurements of the scattered field along a piece of line.

The problem of detecting the target is tackled by analyzing the frequency averaged Wigner-Ville function as applied to the data and does not require any assumption about the signature of the target. We will present two ways of characterizing the target.

The first one is performed using the iterative solution derived from the Newton-Kantorovitch algorithm as applied to the Wigner-Ville function instead of the scattered field as it is usually done. Indeed, if this built-in function is well adapted to the detection of the object and performs a good clutter rejection, our hope is that an inversion procedure based on its optimization allows us to use a forward model involving a flat interface instead of rough surface, the contribution of the latter being considered as noise. Such an approach permits us to save a lot of time since it involves the standard half-space Green's function.

In the second approach we have first used a new type of correlation of the scattered fields in order to obtain an estimation of the surface profile. A direct solver based on a finite element method has been built in order to take into account the reconstruted surface profile. A "level-set" type method coupled with this solver has been used in an iterative process in order to recover the shape of the buried scatterer.

The efficiency of both approaches will be illustrated via numerical experiments and comparisons will be reported.

Non-Destructive Evaluation of Dielectric Structural Materials by Holographic Subsurface Radar

S. Ivashov[1], **V. Razevig**[1], **A. Sheyko**[1], **I. Vasilyev**[1], **and T. Bechtel**[2]

[1]Bauman Moscow State Technical University, Russia
[2]Enviroscan, Inc., USA

The existing methods of non-destructive testing of structural and building materials or components have a number of disadvantages. X-ray devices, for example, require two-way approach to the observed detail. This is complicated sometimes and more often even impossible. X-ray devices are widely used in medicine, for hand-luggage control in airports and in technological processes where two-way approach to the object to be examined has no problems as a rule. Ultrasonic equipment has proved to be ineffective in media containing a great number of micro cracks and heterogeneities. Its main application is the examination of relatively homogeneous media with few defects and inclusions, for example, metal details of relatively large dimensions.

From this point of view, the microwave devices are the most promising as they make possible the use of reflective sounding, i.e., transmission and reception of electromagnetic waves is performed from one side of the sounded surface. It enables to examine walls, ceilings and decorative elements and so on in ready-for-service buildings. Thus, it is possible to control the quality of their construction and repair. When using a specially designed antenna, the proposed method also makes it possible to examine corners between walls. This is hardly possible otherwise. Another advantage of radar sounding is a relatively large wavelength λ in the used microwave band, at which there is no reflection from minor natural heterogeneities of media under investigation, for example, by cracks and small (compared to λ) technological hollows in bricks and other construction materials. By choosing wavelength of emitted signal, it is possible to carry out preliminary selection of heterogeneities in surveyed object in view of features of a task.

However, taking into account that water possesses a very high permittivity of 80, cracks filled with moisture have high contrast. This effect can be used in practice. While constructing and reconstructing, concrete structures or their parts, which are under the level of the construction site ground, have to be sealed to prevent water intrusion. This type of structures includes underground garages, automobile parking places, underground pedestrian crossings, and etc. This problem becomes especially actual in spring and autumn when the soil water level is high.

The recent disastrous loss of Space Shuttle Columbia has aroused the great demand in new methods and devices for non-destructive testing and evaluation of the Space Shuttle Thermal Protection System heat protection tiles, as well as the external fuel tank insulating foam. Various approaches have been suggested for determining the integrity of the tiles and foam. However last flight Space Shuttle Discovery has shown that the difficulties with diagnostics of heat protection system are not overcome till now.

The radar under consideration was originally designed for producing non-destructive microwave images of construction details, buried land mines, and etc. The preliminary investigations indicated that its high resolution and sensitivity to cracks or voids, and variations in the subsurface moisture content of materials under inspection could be useful in providing early warning of hidden, incipient problems in the Shuttle protection systems.

This holographic radar method differs from traditional surface-penetrating radar (which typically uses impulse signals) in the simplicity of equipment design and the considerably smaller aperture of scanning antennae. These innovations allow improvement in the spatial resolution of surface-penetrating radar images. It is noteworthy that the effective detection depth of this method is less than that of traditional impulse radars. Nevertheless, for many applications, the holographic radar will provide sufficient detection depth. A good example is the space shuttle heat protection system, which has tile thickness in the range of 4.3–10 centimeters. Another extremely important advantage of this holographic radar technology is the possibility that it can image, without reverberation, dielectric materials that lie above a metal surface as in case heat protection cover. Such materials cannot effectively be inspected non-destructively with traditional time-domain impulse radar technology.

Some experiments concerning surveying of construction details and foam above metal plate will be presented in full paper.